Delft University of Technology

Real-time pipeline leak detection and localization using an attention-based LSTM approach

Zhang, Xinqi; Shi, Jihao; Yang, Ming; Huang, Xinyan; Usmani, Asif Sohail; Chen, Guoming; Fu, Jianmin; Huang, Jiawei; Li, Junjie

Important note
To cite this publication, please use the final published version (if applicable).
Please check the document version above.

Contents lists available at ScienceDirect

Process Safety and Environmental Protection
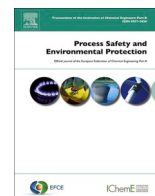
Real-time pipeline leak detection and localization using an attention-based LSTM approach

Xinqi Zhang [a], Jihao Shi [a,b,*], Ming Yang [c], Xinyan Huang [b], Asif Sohail Usmani [b], Guoming Chen [a], Jianmin Fu [a], Jiawei Huang [a], Junjie Li [a]

[a] Centre for Offshore Engineering and Safety Technology, China University of Petroleum, Qingdao 266580, China
[b] Department of Building Environment and Energy Engineering, The Hong Kong Polytechnic University, Kowloon, Hong Kong, China
[c] Safety and Security Science Section, Department of Values, Technology, and Innovation, Faculty of Technology, Policy, and Management, Delft University of Technology, the Netherlands

ARTICLE INFO

ABSTRACT

Long short-term memory (LSTM) has been widely applied to real-time automated natural gas leak detection and localization. However, LSTM approach could not provide the interpretation that this leak position is localized instead of other positions. This study proposes a leakage detection and localization approach by integrating the attention mechanism (AM) with the LSTM network. In this hybrid network, a fully-connected neural network behaving as AM is first applied to assign initial weights to time-series data. LSTM is then used to discover the complex correlation between the weighted data and leakage positions. A labor-scale pipeline leakage experiment of an urban natural gas distribution network is conducted to construct the benchmark dataset. A comparison between the proposed approach and the state-of-the-arts is also performed. The results demonstrate our proposed approach exhibits higher accuracy with AUC = 0.99. Our proposed approach assigns a higher attention weight to the sensor close to the leakage position, indicating the variation of data from the sensor has a significant influence on leakage localization. It corresponds that the closer to the leakage position, the larger variation of monitoring pressure after leakage, which enhances the detection results' trustiness. This study provides a transparent and robust alternative for real-time automatic pipeline leak detection and localization, which contributes to constructing a digital twin of emergency management of urban pipeline leakage.

1. Introduction

The past decade has witnessed significant growth of urban natural gas demand in China (Vairo et al., 2021). Complex natural gas transmission and distribution networks in urban areas have been accordingly constructed, bringing several safety issues. Natural gas leakage from such complex urban pipeline networks is one of the most dangerous events since the released natural gas could accumulate into flammable vapor clouds of large size in urban areas (Zhang et al., 2022). Once being ignited, such vapor clouds would cause fire and explosion accidents resulting in a large number of casualties and significant environmental damage (Shi et al., 2020a, 2022). Real-time pipeline leakage detection and localization are essential to support a quick mitigation decision such as emergency repair strategy to prevent the escalation to fire and explosion disaster (Hassan et al., 2022; Syed et al., 2020).

Research progress has been achieved in developing various kinds of pipeline leakage detection and localization approaches. Model-based approach such as hydraulic gradient approach (Carrera et al., 2015; Lopezlena and Sadovnychiy, 2019; Rojas and Verde, 2020; Torres et al., 2021), Kalman filter approach (Delgado-Aguiñaga et al., 2016, 2021), Fisher Discriminant Analysis approach (Romero-Tapia et al., 2018) etc., has been developed by discovering hidden fluid mechanics with mathematical complexity. Its accuracy of leakage detection and localization

Nomenclature			b	bias vectors in LSTM
			e	Updated probability in LSTM
X	Time-series data		g	Updated value in LSTM
l	Sequence length		U	Cell state in LSTM
N	Number of time series data		O	Output information in LSTM
k	Number of sensors		L	Loss during network training
t	Monitoring time		M	Number of leak positions
c	Weight coefficient		Y	Labels of time-series data
a	Attention weight		TPR	True positive rate
X'	Weighted Time-series data		FPR	False positive rate
$\sigma, \tanh$	Activation function in neural network		TP	True positive sample
f	Output of the forget gate in LSTM		FP	False positive sample
H	Output of LSTM		TN	True negative sample
W	Neural weight in LSTM		FN	False negative sample

for different pipeline networks has been widely accepted as well. In addition, data-driven approach becomes a promising alternative since this approach could directly learn the complex relationship among monitored fluid flow signals in pipelines without knowing the hidden physics and mechanism (Bermúdez et al., 2020; Ye et al., 2021; Korlapati et al., 2022). Quiñones-Grueiro et al. (2018a, 2018b) compared different data-driven approaches for pipeline leakage localization and demonstrated Support Vector Machine (SVM) approach exhibited higher accuracy. Further, Quiñones-Grueiro et al., (2018b) combined a

periodic transformation with principal component analysis (PCA) for leak detection and location in water distribution networks (WDNs). Pérez-Pérez et al. (2021) deployed Artificial Neural Networks (ANN) to estimate the friction factor first and then applied the 2nd ANN for pipeline leakage localization. Irofti et al., (2020, 2022) combined graph-based interpolation and dictionary classification for leak localization in WDNs. Delgado-Aguiñaga et al. (2022) developed an integrated approach based on Nearest Neighbor (KNN) classifier and Extended Kalman Filters (EKFs) for multi-leak detection task in a
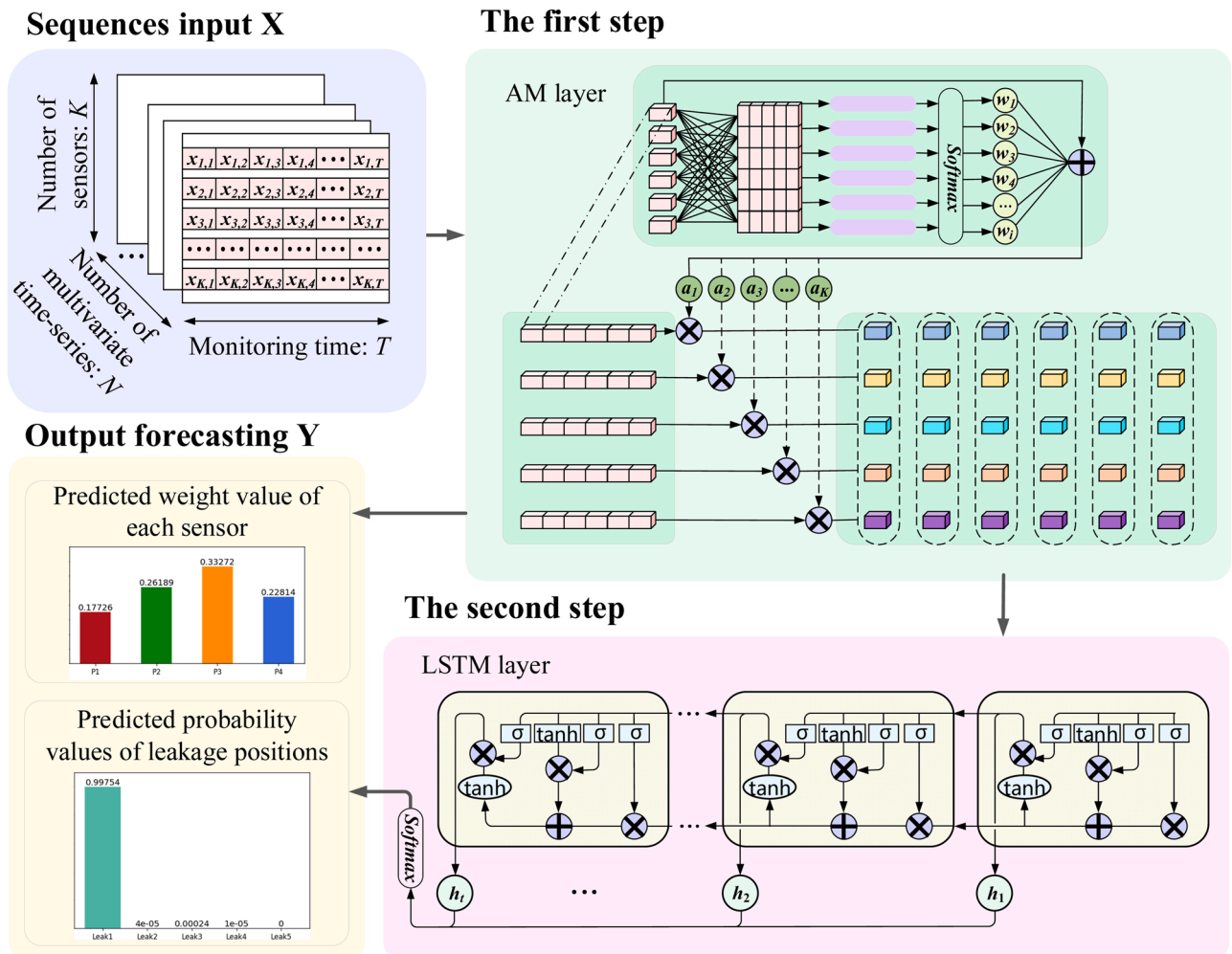

Fig. 1. Architecture of the proposed AM-LSTM approach.

branched pipeline.

The above research works applied machine learning for data-driven approach development. Relatively, deep learning exhibits several advantages in terms of accuracy and efficiency since deep learning could automatedly extract critical features from high-dimension data (Shi et al., 2021, 2023a,b). Romero et al. (2020) applied a deep neural network to classify leakage location by using the image as training data. Kim et al. (2019) applied Long short-term memory (LSTM) to analyze the time-series atmospheric concentration and demonstrated a high accuracy of leakage localization. Spandonidis et al. (2022) applied LSTM-Autoencoder (LSTM-AE) for real-time pipeline leakage detection by automated analyzing monitored time-series signals. However, the above deep learning models behave like a 'black box' and could not provide a reference for automated leakage detection and localization. In this case, attention mechanism (AM) has been applied to improve deep learning's transparency and accuracy for various engineering applications. AM is a feature extraction technique that could enhance features' importance on deep learning performance by assigning larger weights to corresponding features (Jing et al., 2022; Pang et al., 2022; Tian et al., 2022). Yuan et al. (2021) proposed an AM-based approach, Target Transformer, to capture the importance of temporal and spatial features to improve fault diagnoses accuracy in chemical process. Wei et al. (2022) introduced AM into Convolutional Neural Networks (CNNs) and bi-directional long short-term memory (BiLSTM) to explain the contribution proportion of input features for the furnace tube temperature prediction. Gao et al. (2022) cascaded AM to LSTM to give temporal features' contribution while improving prediction accuracy of solar radiation. However, to the best of the authors knowledge, the application of AM to real-time automated pipeline leakage detection and localization has not been explored yet.

This study aims to propose a real-time automated pipeline leakage detection approach by integrating AM with LSTM, namely AM-LSTM, to enhance the trustness of automated leakage detection and localization. Labor-scale leakage experiment in the pipeline with branches is conducted to construct the benchmark dataset. Using such a dataset, a comparison between the proposed and state-of-the-art approaches is also performed. The major contributions and novelty of this study are listed as follows:

(1) A hybrid AM-LSTM approach is developed, in which AM is applied to discover the contribution proportion of each sensor, and LSTM is used to discover the complex correlation between the weighted time-series data and pipeline leakage positions.

(2) An experimental study demonstrates unlike the LSTM-based approach, our proposed approach outputs a higher weight value to the sensor close to the leakage position corresponding to the physical variation of monitoring pressure at the same position, which improves the trustness and robustness of intelligent detection.

(3) The experimental study also demonstrates that our proposed approach exhibits a higher AUC= 0.99 indicating its accuracy in real-time automated pipeline leakage localization compared to the state-of-the-art approaches.

2. The proposed AM-LSTM approach

Fig. 1 demonstrates the architecture of proposed AM-LSTM approach for real-time automated pipeline leakage detection and localization. As can be seen, the AM-LSTM approach consists of two networks, namely a fully-connected neural network and an LSTM network.

The first step of this approach is to feed the time-series dataset X of all sensors into an attention neural network to discover the correlation among each sensor by assigning a weight, which indicates the importance of time-series data from each sensor. The second step is to feed the weighted timing data of different sensors into the LSTM network, which extracts the weighted temporal features and correlates such features to

pipeline leakage positions. By using such integration, the sensor containing the temporal features significantly influencing the location result could be determined by an iteratively adaptive weighting process. Finally, the proposed AM-LSTM will output the weight of each sensor and localize the corresponding leakage position closed to the sensor with higher weight.

1. **The first step** to developing the proposed AM-LSTM-based real-time automated pipeline leakage detection is to construct a multi-time-series dataset from sensors at various positions. The multivariate time-series data X can be expressed as:

$$X = \begin{pmatrix} x_{1,1} & \cdots & x_{1,l} \\ \vdots & \ddots & \vdots \\ x_{k,1} & \cdots & x_{k,l} \end{pmatrix}_N \tag{1}$$

where N is the number of multivariate time series, l is the sequence length, and k is the number of sensors.

The sequence $(x_1, \ldots, x_l)$ from the k-th sensor is first inputted into the fully-connected neural network and calculates a sequence of weight coefficients w_i, which can be expressed as:

$$(c_1, \ldots, c_i) = Softmax(Dense(x_1, \ldots, x_l) = \frac{e^{Dense(x_1,\ldots,x_l)}}{\Sigma_{i=1}^l \exp(Dense(x_1,\ldots,x_l))} \tag{2}$$

where $Softmax$ denotes the activation function, and $Dense$ represents full connected neural network. Furthermore, an attention weight a_k is then calculated by multiplying the weight coefficient of Eq.(2) by sequence $(x_1, \ldots, x_l)$ from the k-th sensor as expressed:

$$a_k = \Sigma_{i=1}^l c_i x_i \tag{3}$$

Then, the sequence $(x_1, \ldots, x_l)$ from the k-th sensor is multiplied by the attention weight a_k to determine the weighted sequence $(x_1, \ldots, x_l)'$ of the k-th sensor as expressed:

$$(x_1, \ldots, x_l)' = (x_1, \ldots, x_l)a_k \tag{4}$$

All the sequences from additional sensors are weighted by using Eqs.(2), (3), (4), (5) to determine all the weighted sequences X' as expressed:

$$X' = \begin{pmatrix} a_1 x_{1,1} & \cdots & a_1 x_{1,l} \\ \vdots & \ddots & \vdots \\ a_k x_{k,1} & \cdots & a_k x_{k,l} \end{pmatrix}_N \tag{5}$$

2. **The second step** is to utilize the LSTM network to learn the temporal information and classify the sequential data. The recurrent Neural Network (RNN) is a commonly used neural network approach for sequence learning problems. As a modified structure of RNN, LSTM adds memory cells into hidden layers to solve the problem of vanishing gradients and exploding gradients in long-sequence learning (Arunthavanathan et al., 2021). The structure of LSTM networks mainly consists of three primary multiplication gates (the forget, input, and output gates) and an update status. Through the switch of gates, memory cells can retain long-term dependencies while excluding invalid information (Li and Wang, 2022; Zhang et al., 2022).

The data fed into the LSTM network is first disposed of by the forget gate, indicating which information of the last moment's cell needs to be discarded. The output of the forget gate f_t at time step t can be expressed as

$$f_t = \sigma(W_f x_t + W_f h_{t-1} + b_f) \tag{6}$$

where σ is the sigmoid function and f_t lies between 0 and 1, x_t is the input
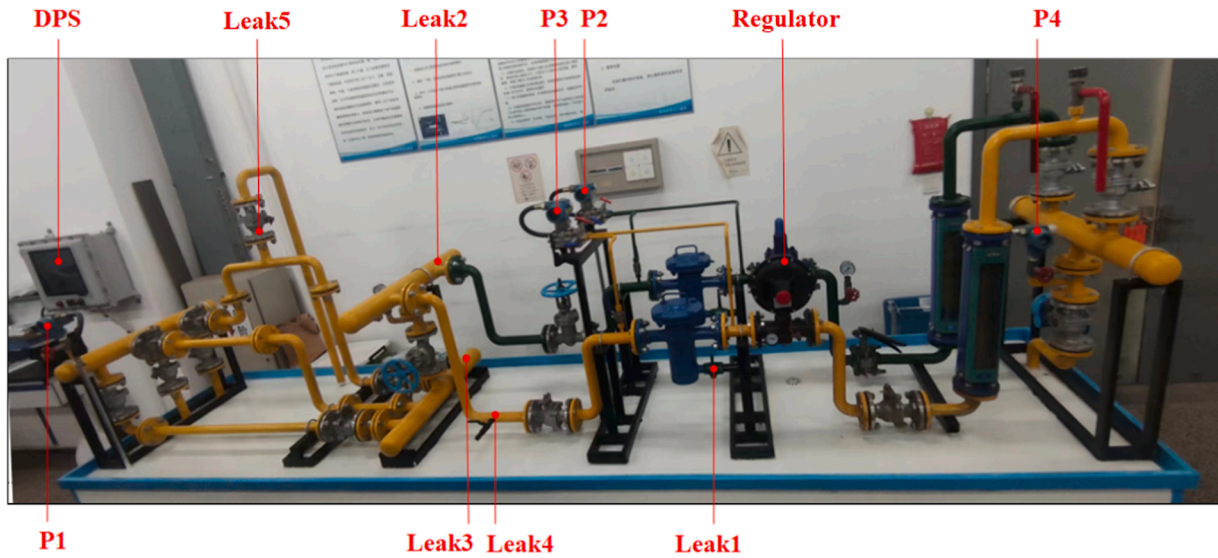
Fig. 2. Labor-scale experimental system of urban gas transmission and distribution pipeline leakage simulation.

of the current time step, h_{t-1} is the output of the previous time step, W_f is the weight, and b_f is the bias vectors.

The input gate determines the information of the current moment which needs to be stored. First, the values need to be updated through the sigmoid function, and the updated probability e_t can be obtained as

$$e_t = \sigma(W_e x_t + W_e h_{t-1} + b_e) \tag{7}$$

Then, a new value g_t is generated to the cell states by the tanh function.

$$g_t = \tanh(W_g x_t + W_g h_{t-1} + b_g) \tag{8}$$

where $\tanh$ is the sigmoid function, W_i and W_g are input weights, b_g, and b_f are bias weights.

Hence, the updated value of the current cell state U_t can be represented as

$$U_t = e_t g_t + f_t \otimes U_{t-1} \tag{9}$$

where U_{t-1} is the previous cell state.

The output gate controls the output information O_t of the current state and the output of the current time h_t.

$$O_t = \sigma(W_o x_t + W_o h_{t-1} + b_o) \tag{10}$$

$$h_t = O_t \otimes \tanh(U_t) \tag{11}$$

By integrating the AM feature extraction network with the LSTM network, the AM-LSTM network is eventually developed. The sparse categorical cross entropy calculated as Eq. (12) is selected as the loss function in the training stage to measure the gap between prediction and actual probability distribution. The loss function will be minimized with the network parameters updated. During training, network parameters can be updated to minimize the loss function by using stochastic gradient descent.

$$L = -1 \bigg/ N \sum_{i=1}^{N} \sum_{j=1}^{M} y_{i,j} \log(\widehat{y}_{i,j}) \tag{12}$$

where L is the loss for M output categories in N input training samples, $y_{i,j}$ and $\widehat{y}_{i,j}$ are the labels of the target and the network's prediction.

After training, the accuracy of classification is then measured by counting the number of correct predictions and dividing by the total number of cases (Kopbayev et al., 2022; Shi et al., 2020b). Given the confusion matrix of the predicted results and the true classification, the

true positive rate (TPR) and the false positive rate (FPR) can be calculated as Eqs. (13) and (14).

$$TPR = \frac{Tp}{TP + FN} \tag{13}$$

$$FPR = \frac{Fp}{FP + TN} \tag{14}$$

where *TP, FP, TN,* and *FN* are true positive, false positive, true negative, and false negative, respectively. Taking FPR as the abscissa and TPR as the ordinate, respectively, the Receiver Operating Characteristic (ROC) curve can be obtained. Then, the network performance is evaluated by the respective Area Under Curve (AUC), as illustrated below:

$$\text{AUC} = \frac{1}{2}\sum_{i}^{N-1}(FPR_{i+1} - FPR_i)\cdot(TPR_i + TPR_{i+1}) \tag{15}$$

Once the network's accuracy is determined, the outputs H of the LSTM units are then sent to the output layer, and the leakage detection result Y_m can be obtained as follows:

$$Y_m = \text{Softmax}(H_m) = \frac{e^{H_m}}{\Sigma_{m=1}^{M}\exp(H_m)} \tag{16}$$

Subsequently, all the sensors are assigned to be the attention weight values by using Eq.(2) and Eq.(3). And the leakage detection result Y_m could be interpreted by using such weight vectors.

3. Benchmark dataset

In this section, a lab-scale gas leakage experiment system of urban gas transmission and distribution pipeline network was applied to simulate various pipeline leakage scenarios. Then, the experimental benchmark matrix containing the time-series data from 4 pressure sensors and 5 labeled leakage positions was constructed for our proposed AM-LSTM approach development.

3.1. Experimental configuration

Fig. 2 demonstrates the lab-scale experiment system of urban gas transmission and distribution pipeline leakage simulation, which was constructed based on a real-world urban gas pipeline network in China. The main component of this experimental system is the central gas pipeline with pipeline branches. The diameter of central gas pipelines is DN80, while the pipeline branches' diameter is DN50. The pipelines

Table 1
Distance from the leakage point to the monitoring sensor.

Leak	Distance to sensor P1/mm	Distance to sensor P2/mm	Distance to sensor P3/mm	Distance to sensor P4/mm
Leak 1	5410	3167	130	3388
Leak 2	3448	2266	2992	5474
Leak 3	2707	3098	3454	6306
Leak 4	4087	3356	1370	4628
Leak 5	1505	4545	4901	7753

meet national safety standards, and the operating pressure is less than 0.8 MPa. A gas regulator and various kinds of valves are installed in the pipeline. The gas regulator is used to adapt the inner pressure of the pipeline ranging from 0.01 to 0.2 MPa, which is set according to the low-pressure transmission and distribution pressure of urban gas. 5 ball valves mounted on the pipeline at 5 positions are applied to generate 5 kinds of gas leakages, namely leak 1, leak 2, leak 3, leak 4, and leak 5. The leakage scenarios and distance between each leakage position and the installed sensor are summarized in Table 1. In addition, pressure signals which are convenient and stable indicators in pipeline leakage diagnosis (Zheng et al., 2020), are used as the time-series signals for pipeline leakage detection. Four pressure sensors denoted as P1, P2, P3, and P4 are mounted along the main pipeline and branches to collect the time-series pressure signals ranging from 0 to 2.5 kPa. Noting that the sensor configurations such as sampling frequency are set according to the Supervisory control and data acquisition system (SCADA) system in real-world urban gas transmission and distribution pipeline networks. Finally, an online data process system (DPS) is applied to collect the online monitoring time-series pressure signals. Using such an experiment system, a total of 500 = 100 * 5 pipeline leakage scenarios are simulated by considering 100 inner pressures adapted by the gas regulator and 5 leakage positions. For each time series pressure signal, the duration is the 60 s with sampling interval= 1 s. Then, we construct the experimental benchmark matrix containing the input matrix $X \in R(60, 4500)$ and the labeled matrix $L \in R(5, 100)$.

3.2. Benchmark dataset processing

Since the experimental pipeline network is composed of pipelines with different pressure grades, i.e., DN50 and DN80, the variation of the monitoring time-series pressure signal among different sensors greatly differs. In this case, data processing is required to ensure all the monitoring data with the same magnitude to accelerate the AM-LSTM network's convergence rate and generalization capability. The min-max normalization is adopted to normalize all the time-series data X between 0 and 1 as expressed (Zheng et al., 2020):

$$x_n = \frac{x_l - x_{min}}{x_{max} - x_{min}} \tag{17}$$

where x_n is the normalized value, x_l is the original value, x_{max} and x_{min} are the maximum and minimum of the original values. After normalization, we further divide the experimental benchmark dataset into two sets, namely the training set (80%) and test set (20%), respectively.

Fig. 3 shows an example of time-series pressure data monitored by 4 sensors under the 1st leakage position, namely leak1. As can be seen, before the leakage occurrence, the monitored pressure fluctuates steadily. However, once leakage is initiated, the pressure drops rapidly. Among all the sensors, the pressure of P3 decreases the most, and the lowest pressure is equal to 0 MPa. This is because P3 is more closed to the leakage position. Once the leakage occurs, the fluid loss at the leakage point will change fluid density near the leakage, resulting in a rapid drop of pressure at the leakage point. The pressure upstream and downstream in the pipeline is greater than the pressure at the leakage point. Driven by the pressure difference, the fluid continues to squeeze to the leakage point, forming a new pressure difference near the leakage point. Subsequently, both the upstream and downstream pressure decrease, resulting in continuous pressure fluctuations. Due to the unavoidable noise in the pipeline network, the pressure fluctuation attenuates with distance and pipeline equipment (Gupta et al., 2018). This results in the smallest drop rate of pressure at P4 due to the fact of P4 is far away from the leakage position. According to such physical phenomena, we may apply our proposed AM-LSTM approach to capture the larger variation of monitoring pressure by the sensor close to the leakage position and thereby assign a higher attention weight to a such sensor, which accordingly enhances the trustiness of real-time automated leakage position identification.

4. Approach development and comparison

4.1. leakage detection and localization

Our proposed AM-LSTM network is constructed using Python version
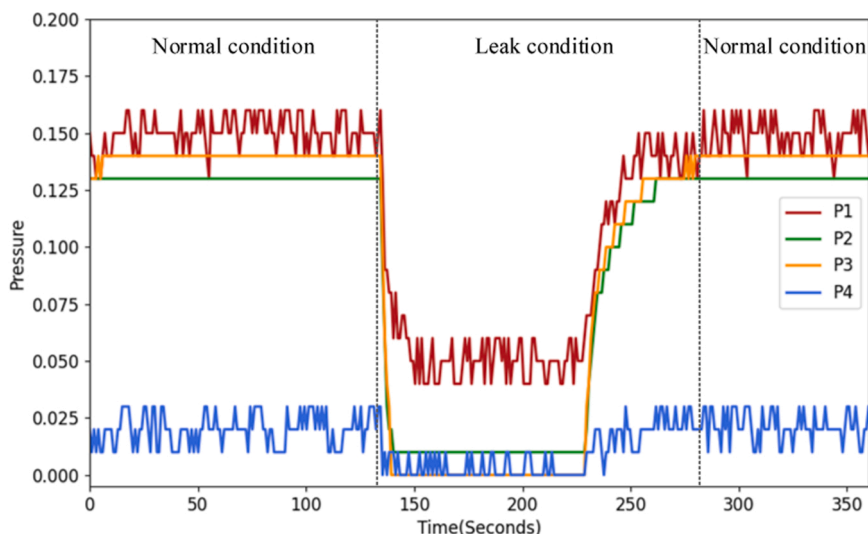
Fig. 3. Time-series pressure data from 4 sensors under inner pressure 0.15 MPa and leak1 (1st leakage position).
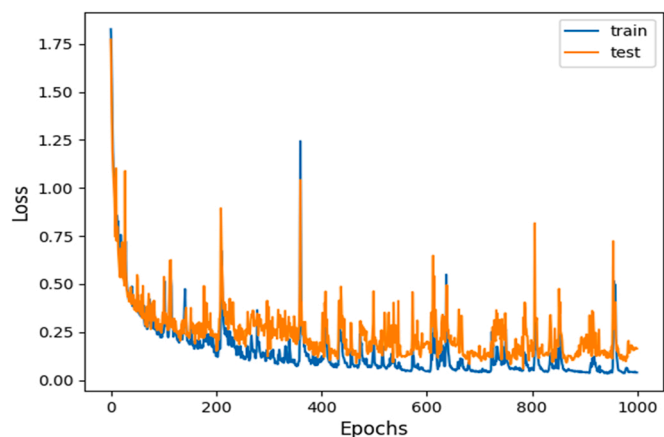
Fig. 4. Loss curves for 1000 epochs generated by AM-LSTM training and testing.

3.10 and the specialized libraries TensorFlow 1.14.0 and Keras 2.3.1. TensorFlow is an open-source platform for machine learning, and Keras is a high-level neural networks application programming interface (API), which can run on top of TensorFlow and enable fast experimentation. Adaptive moment estimation (Adam) is selected as the optimization algorithm to train the network, whose parameters are kept as the default value determined in Keras documentation (Selvaggio et al., 2022). The architecture is composed of AM layer and the LSTM layer. The AM layer adopts 20 dense layers with the activation function of Softmax to calculate the weights, which are then permuted to be multiplied by the input data. The LSTM layer consists of LSTM with 100 hidden units and 5 dense layers with the activation function of Softmax. To prevent overfitting, dropout regularization techniques with a probability of 0.2 and weight decay with a probability of 0.2 are used (Sabiri et al., 2022; Ziv et al., 2021). Fig. 4 demonstrates loss curves for 1000 epochs generated by proposed AM-LSTM training and testing. As can be seen, both training and testing loss curves first decrease rapidly and then become converged after 900 epochs. We thereby select the developed AM-LSTM at 900 epochs for the following analysis.

The monitoring time-series pressure data under operation pressure 0.15 MPa and various leakage positions from the test set is applied to demonstrate the leakage localization ability of the proposed AM-LSTM in terms of real-time automated leakage localization.

a) Predicted probability values of various leakage positions, namely leak1, leak2, leak3, leak4, leak5
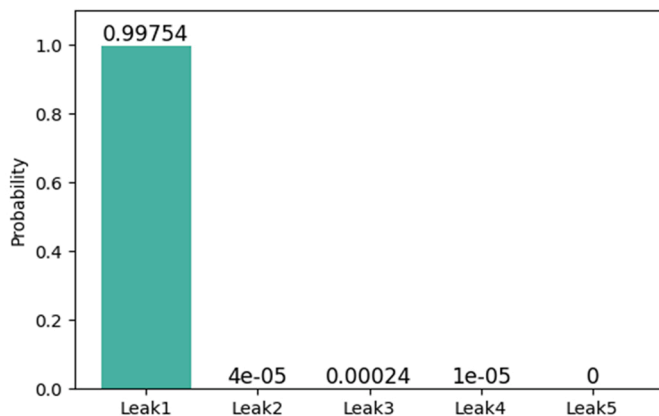
a) Predicted probability values of various leakage positions, namely leak1, leak2, leak3, leak4, leak5
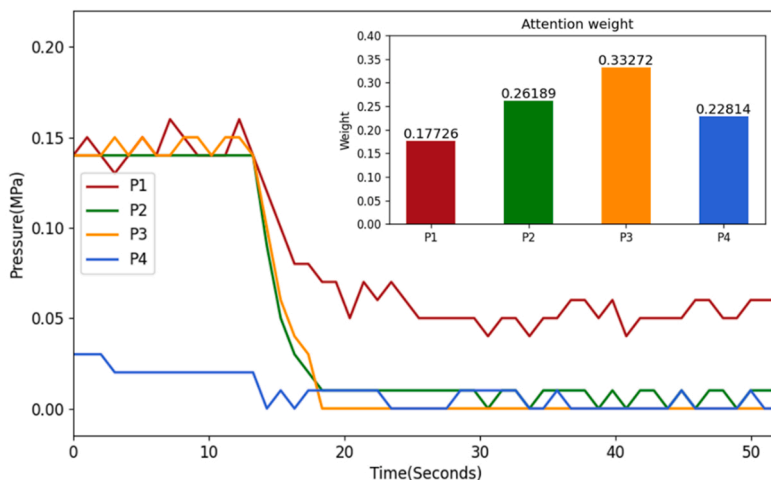
b) Pressure variation by sensors at various positions, i.e., P1, P2, P3, and P4, and the

predicted weight value of each sensor

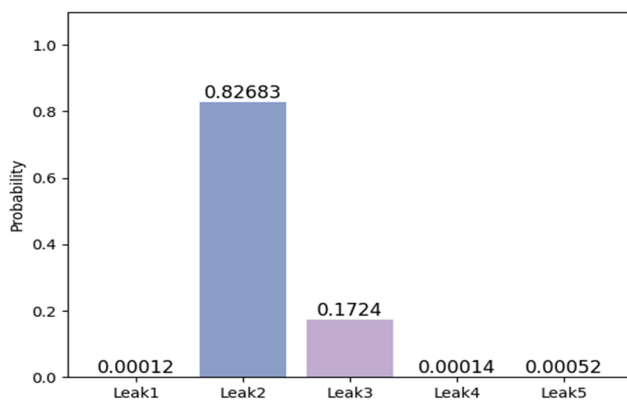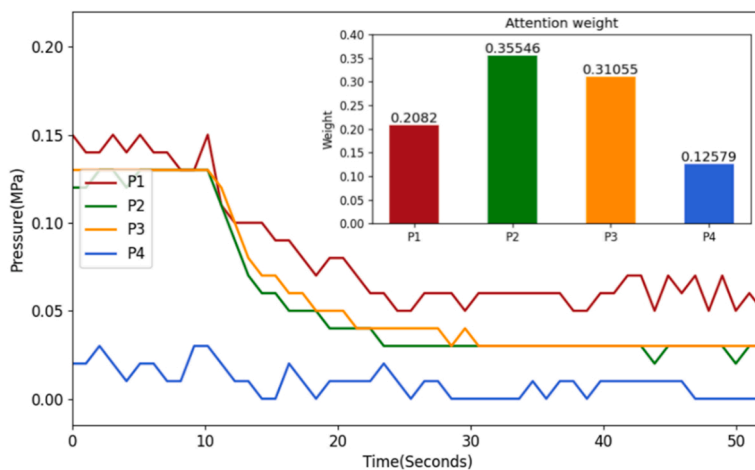**Fig. 5.** Real-time automated leakage detection results under operation pressure 0.15 MPa and leak 1.

a) Predicted probability values of various leakage positions, namely leak1, leak2,

leak3, leak4, leak5

b) Pressure variation by various sensors, i.e., P1, P2, P3, and P4, and predicted weight

value of each sensor

Fig. 6. Real-time automated leakage detection results under operation pressure 0.15 MPa and leak 2.

b) b) Pressure variation by sensors at various positions, i.e., P1, P2, P3, and P4, and the predicted weight value of each sensor

Fig. 5 demonstrates our approach's real-time automated detection results under operation pressure 0.15 MPa and leak 1. Fig. 5a) shows our approach's detection accuracy. As can be seen, the detection probability is 0.99754 under leak 1, which is significantly higher than that under leak 2, leak 3, leak 4, and leak 5. This indicates our approach accurately identifies the actual leakage position. Fig. 5b) demonstrates the time-series pressure data monitored by sensors at various positions, i.e., P1, P2, P3, and P4, and the weight value of each sensor inferred by our approach. From Fig. 5b), one can see once leakage occurs, the pressures monitored by all the sensors have a sudden drop. The pressure by P3 has a larger drop rate than that by P1, P2, and P4. In addition, the pressure by P3 is eventually reduced to 0 MPa. This is because P3 is closer to leak1, which collects a more significant pressure variation. From Fig. 5b), one can also see our approach assigns a larger value of 0.33272 to P3, which indicates our approach can accurately capture the larger physical variation of monitoring pressure by P3. Such higher attention weight enables us to trust the detection result, i.e., detection probability 0.99754 under leak 1.

a) Predicted probability values of various leakage positions, namely leak1, leak2, leak3, leak4, leak5
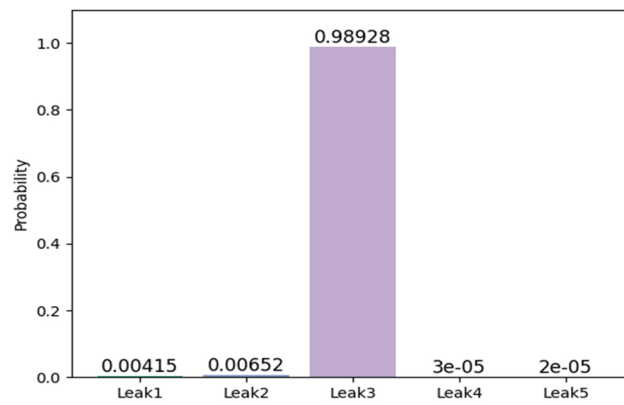
b) b) Pressure variation by various sensors, i.e., P1, P2, P3, and P4, and predicted weight value of each sensor

Fig. 6 demonstrates our approach's real-time automated detection results under operation pressure 0.15 MPa and leak 2. Fig. 6a) demonstrates our approach predicts a higher probability, i.e., 0.82683 under leak2 compared to leak 1, leak 3, leak 4, and leak 5. Fig. 6b) shows the time-series pressure data monitored by sensors at various positions, i.e., P1, P2, P3, and P4, and the weight value of each sensor inferred by our approach. From it, one can see P2 has the higher weight value corresponding to the larger variation of monitoring pressure by P2, which is closer to leakage position 2. Although not predicting a very high probability value, i.e., 0.82683 under leak 2, our approach can convince us to trust the detection result by giving such a higher attention weight to P2.
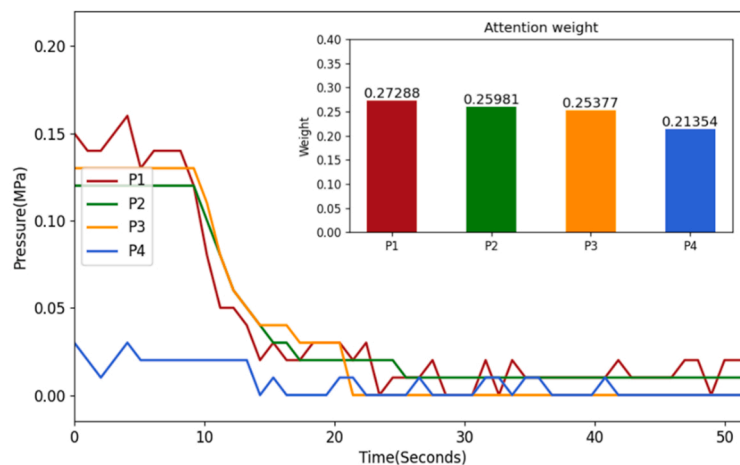
a) Predicted probability values of various leakage positions, namely leak 1, leak 2, leak 3, leak 4, leak 5.

b) Pressure variation by sensors at various positions, i.e., P1, P2, P3, and P4, and the predicted weight value of each sensor.

Fig. 7 demonstrates our approach's real-time automated detection results under operation pressure 0.15 MPa and leak3. Fig. 7a) demonstrates our approach predicts the higher probability, i.e., 0.98928 under leak 3, corresponding to the benchmark leakage position 3. From Fig. 7b), one can see that P1 has the higher weight value, i.e., 0.27288, corresponding to the larger variation of monitoring pressure by P1,

a) Predicted probability values of various leakage positions, namely leak 1, leak 2, leak

3, leak 4, leak 5

b) Pressure variation by sensors at various positions, i.e., P1, P2, P3, and P4, and the

predicted weight value of each sensor

Fig. 7. Real-time automated leakage detection results under operation pressure 0.15 MPa and leak 3.

which is closer to the benchmark leakage position 3. Combining the predicted higher probability, this higher attention weight enables us to trust the identification of leak 3 as the real leakage position.

a) Predicted probability values of various leakage positions, namely leak 1, leak 2, leak 3, leak 4, leak 5.

b) Pressure variation by sensors at various positions, i.e., P1, P2, P3, and P4, and the predicted weight value of each sensor.

Fig. 8 demonstrates our approach's real-time automated detection results under operation pressure 0.15 MPa and leak 4. Fig. 8a) shows our approach predicts the higher probability, i.e., 0.98271 under leak 4 corresponding to the benchmark leakage position 4. From Fig. 8b), one can see P3 has the higher weight value, i.e., 0.36935, corresponding to the larger variation of monitoring pressure by P3, which is closer to the benchmark leakage position 3. Combining the predicted higher probability, this higher attention weight enables us to trust the identification of leak 4 as the real leakage position.

a) Predicted probability values of various leakage positions, namely leak 1, leak 2, leak 3, leak 4, leak 5.

b) Pressure variation by sensors at various positions, i.e., P1, P2, P3, and P4, and the predicted weight value of each sensor.

Fig. 9 demonstrates our approach's real-time automated detection results under operation pressure 0.15 MPa and leak 5. Fig. 9a) shows our approach predicts the higher probability, i.e., 0.99116 under leak 5, corresponding to the benchmark leakage position 5. From Fig. 9b), one

can see that P1 has the higher weight value, i.e., 0.30408, corresponding to the larger variation of monitoring pressure by P1, which is closer to the leakage position 1. This indicates our approach can accurately give the interpretation to identify leak 1 as the real leakage position. Overall, the above detection results verify our proposed AM-LSTM approach not only localizes the accurate leakage position but also gives the interpretation of leakage localization by using the attention weight of each sensor to convince us to trust the detection results.

4.2. Comparison

In this section, a comparison among AM-LSTM, LSTM, and SVM approaches is conducted by using the benchmark test dataset. Fig. 10 demonstrates the ROC curves and AUC values by AM-LSTM, LSTM, and SVM approaches. As can be seen, our proposed AM-LSTM approach exhibits the highest AUC value under each leak position compared to LSTM and SVM approaches. This indicates our proposed approach has superior accuracy for leakage localization, which may be attributed to the additional AM-based network to capture the time-series pressure variation significantly influencing the leakage localization.
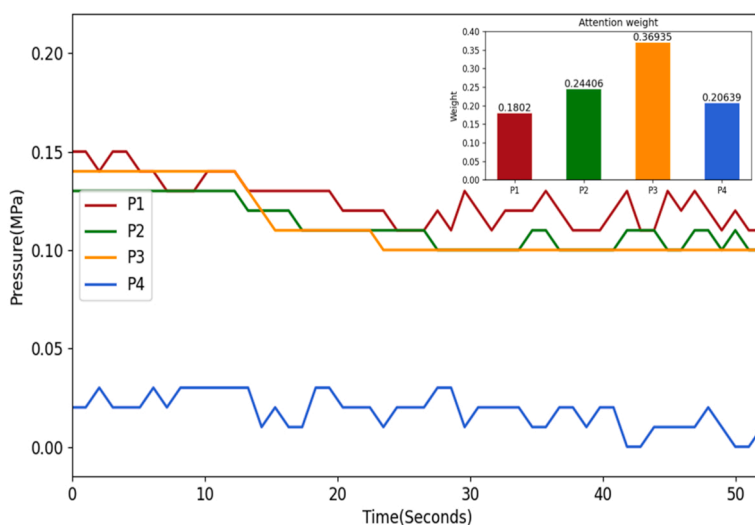
a) ROC curves and AUC values of AM-LSTM.

b) ROC curves and AUC values of LSTM.

c) ROC curves and AUC values of SVM.

Although exhibiting a high AUC value under the whole test dataset,
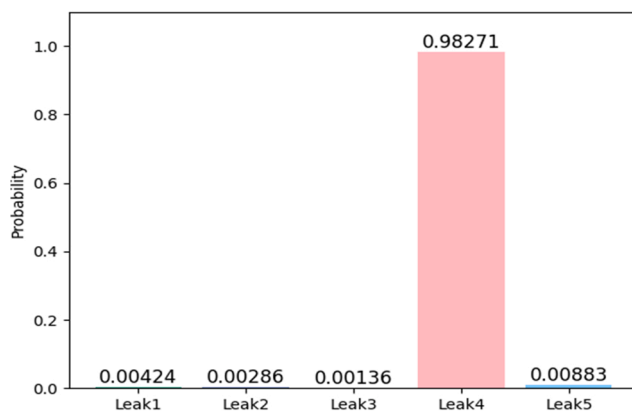
a) Predicted probability values of various leakage positions, namely leak 1, leak 2, leak

3, leak 4, leak 5

b) Pressure variation by sensors at various positions, i.e., P1, P2, P3, and P4, and the

predicted weight value of each sensor

Fig. 8. Real-time automated leakage detection results under operation pressure 0.15 MPa and leak 4.

our proposed approach could still give the misclassification results under some specific leakage position conditions. Examples of operation pressure 0.12 MPa and leakage position 2 (leak 2), operation pressure 0.20 MPa and leakage position 3 (leak 3), and operation pressure 0.17 MPa and leakage position 5 (leak 5) are demonstrated. Table 2 shows the misclassified results under the example leakage conditions. Fig. 11 illustrates the assigned attention weight to 4 sensors, P1 to P4, under the same leakage condition as the example. As can be seen under leak 2 scenario, our approach incorrectly localizes the leakage position as leak 5. And our approach assigns the highest weight value to P4, which is far from the localized leakage position 5 compared to other sensors. This means inconsistency exists between the leakage position identification and its interpretation, which suggests our approach predicts unreliable detection results under the leak 2 scenario. In addition, for leak 3 and leak 5 scenarios, inconsistencies exist between the leakage localization and its interpretation. For example, under leak 3 scenario, our approach incorrectly localizes the leakage position as leak 2. However, our approach assigns the highest weight value to P3 rather than P2, which is the closest sensor from position of leak 2. This inconsistency could be used as the reference to avoid leakage position misclassification induced by LSTM approach without considering AM. Overall, our proposed AM-LSTM approach has been verified more accurate and reliable

for pipeline leakage detection and localization compared to traditional data-driven approaches.

a) Benchmark leakage position 2, namely leak 2.
b) Benchmark leakage position 3, namely leak 3.
c) Benchmark leakage position 5, namely leak 5.

5. Discussions

Although exhibiting higher performance compared to traditional data-driven approach, our proposed AM-LSTM approach still has some limitations as follows:

(1) Our proposed AM-LSTM approach is suitable for leakage condition with medium or high leak rate. Under this condition, the variation of monitored pressure signals is larger compared to that under the condition with low-rate leak. In addition, our AM-LSTM approach is developed by using the monitored signals from labor-scale experimental system and thereby could not be directly applied for real-world full-scale urban pipeline network. The scale ranging from labor to real-world pipeline network is a significant factor to affect our proposed approach's performance. For potential real-world applications, it is suggested to arrange sensors in the main pipeline and each pipeline branch. Also, further works are expected to investigate the scale effect
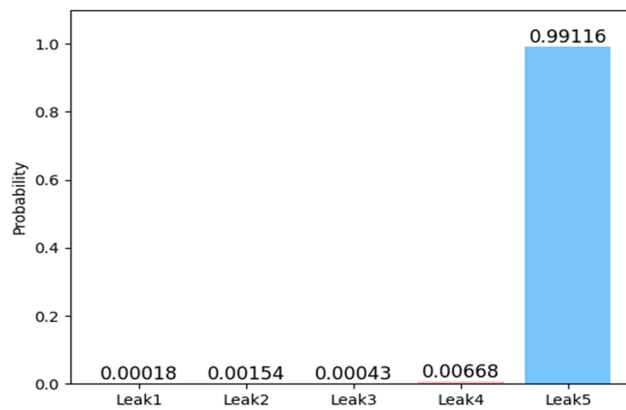
a) Predicted probability values of various leakage positions, namely leak 1, leak 2, leak

3, leak 4, leak 5
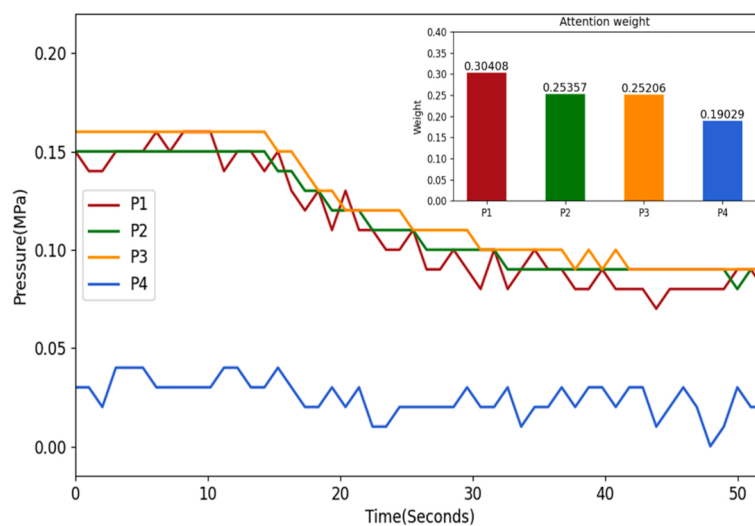
b) Pressure variation by sensors at various positions, i.e., P1, P2, P3, and P4, and the

predicted weight value of each sensor

Fig. 9. Real-time automated leakage detection results under operation pressure 0.15 MPa and leak 5.

on this approach's performance for leakage detection and localization.

(2) Our proposed AM-LSTM is a supervised machine learning approach, which requires a large number of labeled leakage data for model training. For real-world applications, such labeled anomaly data is difficult to be collected and the proposed approach's performance would be certainly harmed. This is a tough but interesting topic. Expected solutions may include *[1]* scaling such supervised model to real-world applications with few labeled leak data or without any labeled leak data by using a domain adaptive transfer learning approach, *[2]* probabilistic unsupervised machine learning, and *[3]* physics-informed machine learning approaches, etc. For model training, for example, solution *[1]*, one may train a machine learning model by using labor-scale experimental leakage data at the 1st step and then scale such model with desirable accuracy to real-world pipeline network by using normal monitored time-series data and domain adaptive transfer learning approach.

(3) Our proposed AM-LSTM is one of data-driven approaches for pipeline leakage detection and localization. Compared to model-based approaches, our approach's advantage is that one may not necessarily know the hidden physics regarding pipeline geometry, fluid, pressure, etc., while directly using the monitored data for model training for pipeline leakage detection. Please noting such monitored data is from

the pipeline network itself and somehow includes the hidden physics regarding the pipeline network. However, if the network configuration is changed, the developed model's performance would be harmed. One may collect new data from the changed pipeline network and re-train this developed model. This is another limitation of our proposed approach. Further work is expected to improve the generalization of our proposed approach for real-world applications.

6. Conclusions

This study proposed an attention mechanism-long short-term memory (AM-LSTM)-based approach for a single leak location in a branched pipeline network. The experimental study is constructed to demonstrate the accuracy and interpretation of the proposed approach. The conclusions are as follows:
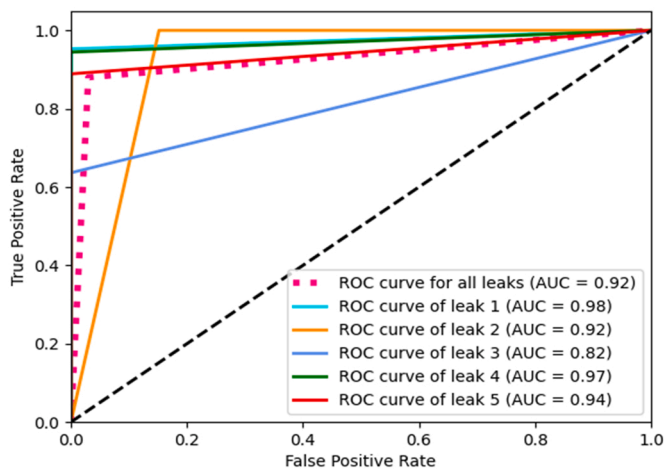
(1) The proposed approach accurately captures the larger physical pressure variation detected by the sensors closer to the leakage position. Accordingly, it assigns a higher attention weight to these sensors to enhance the trustiness and robustness of intelligent localization.
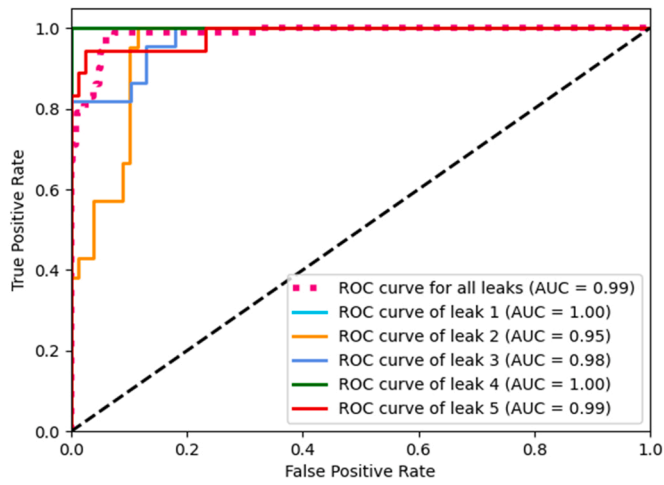
a) ROC curves and AUC values of AM-LSTM
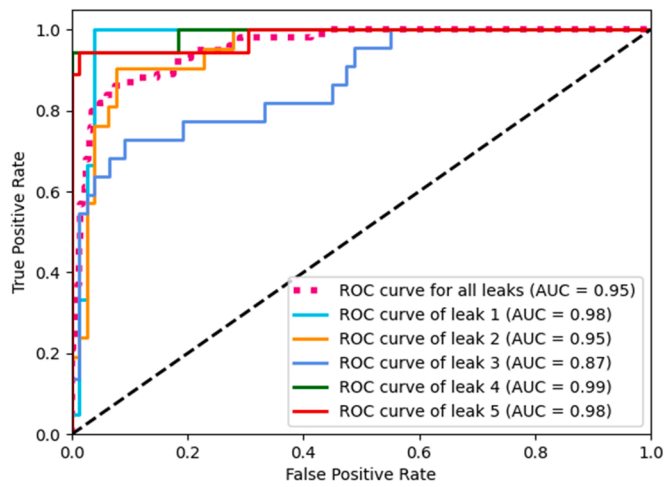

b) ROC curves and AUC values of LSTM

c) ROC curves and AUC values of SVM

**Fig. 10.** Accuracy comparison between our proposed AM-LSTM and LSTM approaches.

(2) The proposed approach exhibits a higher AUC= 0.99 indicating its accuracy in real-time automated pipeline leakage localization compared to the LSTM-based approach.

(3) For misclassification cases, the proposed approach shows the contradiction between assigned attention weight and detection

Table 2

Misclassified results under various leakage conditions.

Operation pressure	Benchmark label	Predicted label	Sensor closest to leak point	Sensor with the highest weight
0.12 MPa	Leak2	Leak5	P1	P4
0.20 MPa	Leak3	Leak2	P2	P3
0.17 MPa	Leak5	Leak4	P3	P2
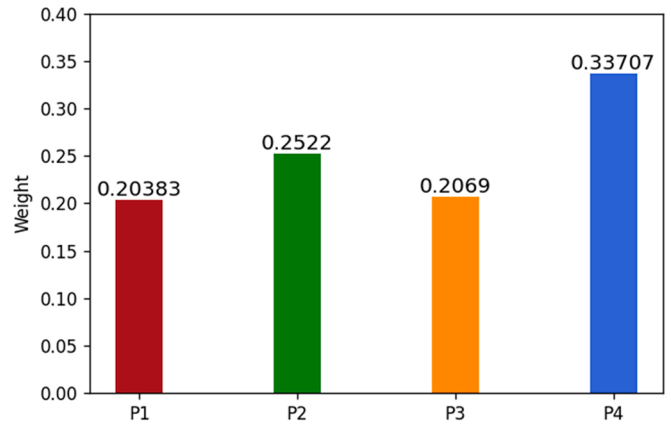
a) Benchmark leakage position 2, namely leak 2
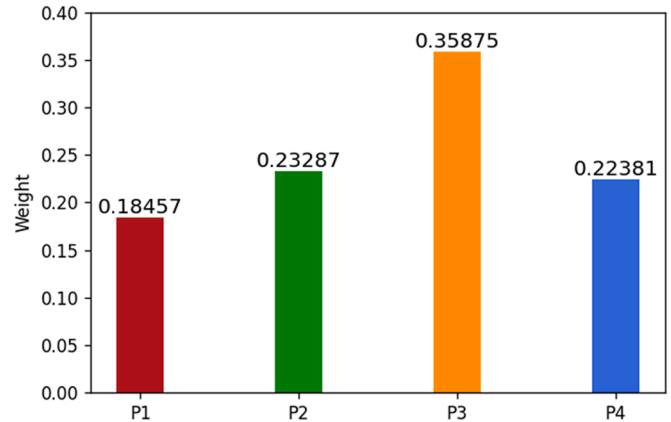
b) Benchmark leakage position 3, namely leak 3
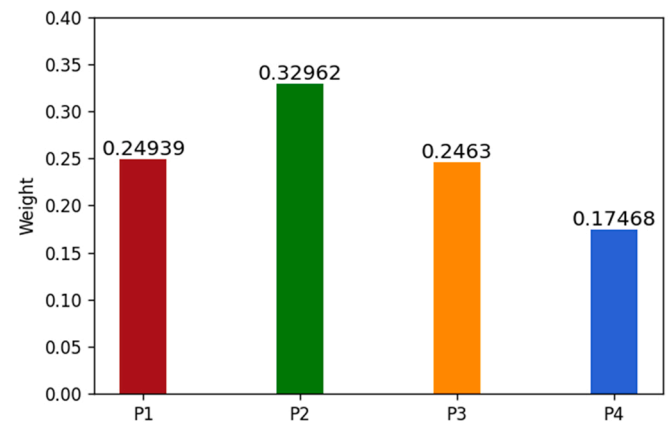
c) Benchmark leakage position 5, namely leak 5

Fig. 11. Attention weights to 4 sensors, namely P1 to P4, under the same benchmark leakage conditions as in Table2.

probability and thereby convinces not to trust these detection results, indicating its higher reliability compared to the state-of-the-art approaches.

Declaration of Competing Interest

The authors declare that they have no known competing financial interests or personal relationships that could have appeared to influence the work reported in this paper.

Acknowledgments

References

Arunthavanathan, R., Khan, F., Ahmed, S., Imtiaz, S., 2021. A deep learning model for process fault prognosis. Process Saf. Environ. Prot. 154, 467–479. https://doi.org/10.1016/j.psep.2021.08.022.

Bermúdez, J.R., López-Estrada, F.R., Besançon, G., Torres, L., Santos-Ruiz, I., 2020. Leak-Diagnosis Approach for Water Distribution Networks based on a k-NN classification algorithm. IFAC-Pap. 53, 16651–16656. https://doi.org/10.1016/j.ifacol.2020.12.795.

Carrera, R., Verde, C., Cayetano, R., 2015. A SCADA expansion for leak detection in a pipeline. CEUR Workshop Proc. 145–152.

Delgado-Aguiñaga, J.A., Puig, V., Becerra-López, F.I., 2021. Leak diagnosis in pipelines based on a Kalman filter for linear parameter varying systems. Control Eng. Pract. 115, 104888 https://doi.org/10.1016/j.conengprac.2021.104888.

Delgado-Aguiñaga, J.A., Besançon, G., Begovich, O., Carvajal, J.E., 2016. Multi-leak diagnosis in pipelines based on Extended Kalman Filter. Control Eng. Pract. 49, 139–148. https://doi.org/10.1016/j.conengprac.2015.10.008.

Delgado-Aguiñaga, J.A., Santos-Ruiz, I., Besançon, G., López-Estrada, F.R., Puig, V., 2022. EKF-based observers for multi-leak diagnosis in branched pipeline systems. Mech. Syst. Signal Process. 178, 109198 https://doi.org/10.1016/j.ymssp.2022.109198.

Gao, Y., Miyata, S., Akashi, Y., 2022. Interpretable deep learning models for hourly solar radiation prediction based on graph neural network and attention. Appl. Energy 321, 119288. https://doi.org/10.1016/j.apenergy.2022.119288.

Gupta, P., Thein Zan, T.T., Wang, M., Dauwels, J., Ukil, A., 2018. Leak detection in low-pressure gas distribution networks by probabilistic methods. J. Nat. Gas. Sci. Eng. 58, 69–79. https://doi.org/10.1016/j.jngse.2018.07.012.

Hassan, S., Wang, J., Kontovas, C., Bashir, M., 2022. An assessment of causes and failure likelihood of cross-country pipelines under uncertainty using bayesian networks. Reliab. Eng. Syst. Saf. 218, 108171 https://doi.org/10.1016/j.ress.2021.108171.

Irofti, P., Stoican, F., Puig, V., 2020. Fault handling in large water networks with online dictionary learning. J. Process Control 94, 46–57. https://doi.org/10.1016/j.jprocont.2020.08.003.

Irofti, P., Romero-Ben, L., Stoican, F., Puig, V., 2022. Data-driven leak localization in water distribution networks via dictionary learning and graph-based interpolation. 2022 IEEE Conf. Control Technol. Appl. CCTA 2022, 1265–1270. https://doi.org/10.1109/CCTA49430.2022.9966160.

Jing, S., Liu, X., Gong, X., Tang, Y., Xiong, G., Liu, S., Xiang, S., Bi, R., 2022. Correlation analysis and text classification of chemical accident cases based on word embedding. Process Saf. Environ. Prot. 158, 698–710. https://doi.org/10.1016/j.psep.2021.12.038.

Kim, H., Park, M., Kim, C.W., Shin, D., 2019. Source localization for hazardous material release in an outdoor chemical plant via a combination of LSTM-RNN and CFD simulation. Comput. Chem. Eng. 125, 476–489. https://doi.org/10.1016/j.compchemeng.2019.03.012.

Kopbayev, A., Khan, F., Yang, M., Halim, S.Z., 2022. Gas leakage detection using spatial and temporal neural network model. Process Saf. Environ. Prot. 160, 968–975. https://doi.org/10.1016/j.psep.2022.03.002.

Korlapati, N.V.S., Khan, F., Noor, Q., Mirza, S., Vaddiraju, S., 2022. Review and analysis of pipeline leak detection methods. J. Pipeline Sci. Eng. 2. https://doi.org/10.1016/j.jpse.2022.100074.

Li, M., Wang, Z., 2022. LSTM-augmented deep networks for time-variant reliability assessment of dynamic systems. Reliab. Eng. Syst. Saf. 217, 108014 https://doi.org/10.1016/j.ress.2021.108014.

Lopezlena, R., Sadovnychiy, S., 2019. Pipeline leak detection and location using boundary feedback estimation: case study. J. Pipeline Syst. Eng. Pr. 10. https://doi.org/10.1061/(asce)ps.1949-1204.0000382.

Pang, C., Duan, D., Zhou, Z., Han, S., Yao, L., Zheng, C., Yang, J., Gao, X., 2022. An integrated LSTM-AM and SPRT method for fault early detection of forced-oxidation system in wet flue gas desulfurization. Process Saf. Environ. Prot. 160, 242–254. https://doi.org/10.1016/j.psep.2022.01.062.

Pérez-Pérez, E.J., López-Estrada, F.R., Valencia-Palomo, G., Torres, L., Puig, V., Mina-Antonio, J.D., 2021. Leak diagnosis in pipelines using a combined artificial neural network approach. Control Eng. Pract. 107, 104677 https://doi.org/10.1016/j.conengprac.2020.104677.

Quiñones-Grueiro, M., Verde, C., Prieto-Moreno, A., Llanes-Santiago, O., 2018b. An unsupervised approach to leak detection and location in water distribution networks. Int. J. Appl. Math. Comput. Sci. 28, 283–295. https://doi.org/10.2478/amcs-2018-0020.

Quiñones-Grueiro, M., Bernal-de Lázaro, J.M., Verde, C., Prieto-Moreno, A., Llanes-Santiago, O., 2018a. Comp. Classif. Leak. Locat. Water Distrib. Netw. * 407–413. https://doi.org/10.1016/j.ifacol.2018.09.609.

Rojas, J., Verde, C., 2020. Adaptive estimation of the hydraulic gradient for the location of multiple leaks in pipelines. Control Eng. Pract. 95, 104226 https://doi.org/10.1016/j.conengprac.2019.104226.

Romero, L., Blesa, J., Puig, V., Cembrano, G., Trapiello, C., 2020. First results in leak localization in water distribution networks using graph-based clustering and deep learning. IFAC-Pap. 53, 16691–16696. https://doi.org/10.1016/j.ifacol.2020.12.1104.

Romero-Tapia, G., Fuente, M.J., Puig, V., 2018. Leak localization in water distribution networks using fisher discriminant analysis. IFAC-Pap. 51, 929–934. https://doi.org/10.1016/j.ifacol.2018.09.686.

Sabiri, B., El Asri, B., Rhanoui, M., 2022. Mechanism of overfitting avoidance techniques for training deep neural networks. Proc. 24th Int. Conf. Enterp. Inf. Syst. 418–427. https://doi.org/10.5220/0011114900003179.

Selvaggio, A.Z., Sousa, F.M.M., Silva, F.V., da, Vianna, S.S.V., 2022. Application of long short-term memory recurrent neural networks for localisation of leak source using 3D computational fluid dynamics. Process Saf. Environ. Prot. 159, 757–767. https://doi.org/10.1016/j.psep.2022.01.021.

Shi, J., Chang, Y., Khan, F., Zhu, Y., Chen, G., 2020a. Methodological improvements in the risk analysis of an urban hydrogen fueling station. J. Clean. Prod. 257, 120545. https://doi.org/10.1016/j.jclepro.2020.120545.

Shi, J., Chang, Y., Xu, C., Khan, F., Chen, G., Li, C., 2020b. Real-time leak detection using an infrared camera and Faster R-CNN technique. Comput. Chem. Eng. 135 https://doi.org/10.1016/j.compchemeng.2020.106780.

Shi, J., Li, J., Usmani, A.S., Zhu, Y., Chen, G., Yang, D., 2021. Probabilistic real-time deep-water natural gas hydrate dispersion modeling by using a novel hybrid deep learning approach. Energy 219, 119572. https://doi.org/10.1016/j.energy.2020.119572.

Shi, J., Zhang, H., Li, J., Xie, W., Zhao, W., Usmani, A.S., Chen, G., 2023b. Real-time natural gas explosion modeling of offshore platforms by using deep learning probability approach. Ocean Eng 276, 114244. https://doi.org/10.1016/j.oceaneng.2023.114244.

Shi, J., Xie, W., Huang, X., Xiao, F., Usmani, A.S., Khan, F., Yin, X., Chen, G., 2022. Real-time natural gas release forecasting by using physics-guided deep learning probability model. J. Clean. Prod. 368, 133201 https://doi.org/10.1016/j.jclepro.2022.133201.

Shi, J., Xie, W., Li, J., Zhang, X., Huang, X., Usmani, A.S., Khan, F., Chen, G., 2023a. Real-time plume tracking using transfer learning approach. Comput. Chem. Eng. 172, 108172. https://doi.org/10.1016/j.compchemeng.2023.108172.

Spandonidis, C., Theodoropoulos, P., Giannopoulos, F., Galiatsatos, N., Petsa, A., 2022. Evaluation of deep learning approaches for oil & gas pipeline leak detection using wireless sensor networks. Eng. Appl. Artif. Intell. 113, 104890 https://doi.org/10.1016/j.engappai.2022.104890.

Syed, M.M., Lemma, T.A., Vandrangi, S.K., Ofei, T.N., 2020. Recent developments in model-based fault detection and diagnostics of gas pipelines under transient conditions. J. Nat. Gas. Sci. Eng. 83, 103550 https://doi.org/10.1016/j.jngse.2020.103550.

Tian, C., Niu, T., Wei, W., 2022. Developing a wind power forecasting system based on deep learning with attention mechanism. Energy 257, 124750. https://doi.org/10.1016/j.energy.2022.124750.

Torres, L., Verde, C., Molina, L., 2021. Leak diagnosis for pipelines with multiple branches based on model similarity. J. Process Control 99, 41–53. https://doi.org/10.1016/j.jprocont.2020.12.003.

Vairo, T., Pontiggia, M., Fabiano, B., 2021. Critical aspects of natural gas pipelines risk assessments. A case-study application on buried layout. Process Saf. Environ. Prot. 149, 258–268. https://doi.org/10.1016/j.psep.2020.10.050.

Wei, Z., Ji, X., Zhou, L., Dang, Y., Dai, Y., 2022. A novel deep learning model based on target transformer for fault diagnosis of chemical process. Process Saf. Environ. Prot. 167, 480–492. https://doi.org/10.1016/j.psep.2022.09.039.

Ye, K., Tang, X., Zheng, Y., Ju, X., Peng, Y., Liu, H., Wang, D., Cao, B., Yang, L., 2021. Estimating the two-dimensional thermal environment generated by strong fire plumes in an urban utility tunnel. Process Saf. Environ. Prot. 148, 737–750. https://doi.org/10.1016/j.psep.2021.01.030.

Yuan, Z., Yang, Z., Ling, Y., Wu, C., Li, C., 2021. Spatiotemporal attention mechanism-based deep network for critical parameters prediction in chemical process. Process Saf. Environ. Prot. 155, 401–414. https://doi.org/10.1016/j.psep.2021.09.024.

Zhang, C., Hu, D., Yang, T., 2022. Anomaly detection and diagnosis for wind turbines using long short-term memory-based stacked denoising autoencoders and XGBoost. Reliab. Eng. Syst. Saf. 222. https://doi.org/10.1016/j.ress.2022.108445.

Zhang, X., Chen, G., Yang, D., He, R., Zhu, J., Jiang, S., Huang, J., 2022. A novel resilience modeling method for community system considering natural gas leakage evolution. Process Saf. Environ. Prot. 168, 846–857. https://doi.org/10.1016/j.psep.2022.10.030.

Zheng, J., Dai, Y., Liang, Y., Liao, Q., Zhang, H., 2020. An online real-time estimation tool of leakage parameters for hazardous liquid pipelines. Int. J. Crit. Infrastruct. Prot. 31. https://doi.org/10.1016/j.ijcip.2020.100389.

Ziv, Y., Goldberger, J., Riklin Raviv, T., 2021. Stochastic weight pruning and the role of regularization in shaping network structure. Neurocomputing 462, 555–567. https://doi.org/10.1016/j.neucom.2021.08.007.